

Comparison Between Digital Radiography and Computed Tomography for the Detection of Metal Fragments in Postmortem Examined Pinniped Skulls

Victoria Sorriba,^{1,2} Lia Lujan,¹ Viviana De los Santos,¹ Adam W. Stern,³ Federico R. Vilaplana Grosso,⁴ and Juan Pablo Damián⁵

¹Escuela Universitaria de Tecnología Médica, Facultad de Medicina, Universidad de la República–Uruguay
E-mail: victoriasorriba@gmail.com

²Departamento de Clínicas y Hospital Veterinario, Facultad de Veterinaria, Universidad de la República–Uruguay

³Department of Comparative, Diagnostic, and Population Medicine,
College of Veterinary Medicine, University of Florida, USA

⁴Department of Small Animal Clinical Sciences, College of Veterinary Medicine, University of Florida, USA

⁵Departamento de Biociencias Veterinarias, Facultad de Veterinaria, Universidad de la República–Uruguay

Abstract

The conservation of marine animals, such as pinnipeds, is very difficult when their feeding areas overlap with fishing activity. During these interactions, they are often victims of firearm injuries that result in their death. For veterinarians and biologists investigating crimes against wildlife, the use of diagnostic imaging techniques is essential. Although computed tomography (CT) can be used to evaluate animals with skeletal trauma, digital radiography (DR) is a cheaper and more widely available diagnostic imaging technique. The objective of this study was to determine whether the presence and number of metal fragments in the skull of pinnipeds differed between DR and CT. Thirty pinniped skulls—19 South American sea lions (*Otaria byronia*) and 11 South American fur seals (*Arctocephalus australis*)—with evidence of trauma and available DR and CT examinations were included in the study. The DR and CT images were evaluated by three independent observers—a veterinarian, a board-certified veterinary pathologist, and a board-certified veterinary radiologist. The detection of metal fragments in pinniped skulls with both imaging techniques was not different between the observers ($p = 1.0$), and it was not significantly different between DR (13/30) and CT (16/30) ($p = 0.71$). The number of metal fragments in pinniped skulls was also not significantly different between DR (6.6 ± 1.9) and CT (7.9 ± 1.7) ($p = 0.37$). Furthermore, there was excellent agreement between the three observers in the detection and number of fragments both for DR (kappa = 1.0; $p < 0.0001$) and for CT (kappa = 1.0; $p < 0.0001$), as well as between the two techniques (DR and CT: kappa = 0.802; $p < 0.0001$). This study showed that CT identified more skulls with metal

fragments and an increased number of metal fragments as compared to DR; however, there were no significant statistical differences noted, suggesting that DR is just as useful as CT for the detection of metal fragments in pinniped skulls. Therefore, DR is a valid tool that can be used to investigate cases of projectile injuries against wildlife.

Key Words: gunshot injuries, projectile injuries, sea lion, seal, metal fragment, diagnostic imaging, head trauma

Introduction

Some of the main causes of anthropogenic mortality in pinnipeds (i.e., seals, sea lions, fur seals, and walrus) are the destruction of their breeding areas and interactions with industrial and artisanal fishing fleets where they may be killed by firearms or explosives (Cárdenas, 2018). The most common and abundant pinnipeds in South America belong to two species, both belonging to the Otariidae family: the South American sea lion or maned seal (*Otaria byronia*; Blainville, 1820) and the South American fur seal or common fur seal (*Arctocephalus australis*; Zimmermann, 1783) (Bastida & Rodríguez, 2010; Jefferson et al., 2015). In Uruguay, the main cause of death in both species is human-induced wounds or injuries, largely due to the close proximity of feeding areas to fishing activity (Crespo et al., 2012). Traumatic injuries in marine mammals can be difficult to investigate because these events occur at sea without witnesses and often there is significant decomposition and evidence of scavenging. Despite this, the differentiation between natural and anthropogenic causes of death is

often possible (Read & Murray, 2000). Forensic veterinary medicine is a developing science different to human forensic medicine because of the number of animal species and the amount of anatomical variables (Newbery & Munro, 2011; Munro & Munro, 2013). Radiography complements the autopsy, particularly in cases of death due to violence, with wildlife being one of the most vulnerable animal populations (Ribas et al., 2015). Before analyzing a deceased human, the most commonly utilized imaging techniques are radiography and computed tomography (CT) as these techniques both allow for the detection of many types of projectiles present in tissues and organs (Stein et al., 2000; Montes Loaiza et al., 2013; Listos et al., 2016; Watson, 2018), and the detection of fractures when the morphology of the wounds makes it difficult to identify the lesion (Di Maio, 2015; Watson & Heng, 2017). These imaging techniques allow veterinarians and biologists to have additional tools available to make diagnoses and to determine the potential cause of death in animals being examined (Singal, 2015).

Although digital radiography (DR) and CT are non-invasive techniques and do not require manipulation or destruction of the animal being examined, there are differences between these modalities. DR generates a two-dimensional image, limiting the evaluation of the trajectory of wounds and injuries (Brogdon, 1998). On the other hand, CT allows the observer to examine the interior of the body (Aso et al., 2005) through many different types of reconstructions, including in various planes (Harcke et al., 2007; Thali et al., 2007; Motta-Ramírez et al., 2013). Use of CT can reveal patterns of fractures as a result of a projectile passing through the bone (Jeffery et al., 2008), as well as identification of old injuries (Montes Loaiza et al., 2013).

For veterinarians, forensic investigators, and biologists, access to advanced diagnostic imaging modalities such as CT to investigate the presence of metal fragments in the body or skeletal remains of animals can become expensive, and equipment is often inaccessible, particularly in remote locations. However, despite being a cheaper and more accessible modality, DR is most commonly used in veterinary medicine. The objective of this study was to compare the sensitivity of DR and CT to determine the presence and number of metal fragments in pinniped skulls. We hypothesize that DR would be as sensitive as CT in the detection of metal fragments, as well as in identifying the number of fragments.

Methods

Pinniped Skulls

In this study, 30 pinniped skulls, including *Otaria byronia* ($n = 19$) and *Arctocephalus australis* ($n = 11$), were examined. All skulls were found on the oceanic coasts of Uruguay and belong to the Museo Nacional de Historia Natural del Uruguay (National Natural History Museum of Uruguay). This institution authorized the Escuela Universitaria de Tecnología Médica of Montevideo, Uruguay, to use the skulls for this study. These skulls were evaluated by the Uruguayan forensic technical police and determined to have evidence of traumatic bone injuries. Given the absence of the mandibles in several of the skulls, this region was not assessed when reporting the presence and number of metal fragments. Prior to analysis, each skull was assigned a random number to be used to identify the samples.

Imaging Studies

Digital Radiography—The DR examination of the samples was carried out using a Vetter Rems (300 mA/125 kV; Monoblock, Buenos Aires, Argentina) x-ray tube and a Kodak Direct View digitizer automatic processor (SRX-101A; Carestream Health Inc., Rochester, NY, USA). The skulls were positioned in ventral (Figure 1) and right lateral (Figure 2) recumbency. Image detectors of 35 × 43 cm and 24 × 30 cm were used depending on the size of the skull. In cases where it was necessary, radiolucent sponges were used to position the skulls. The radiographic technique settings used were variable, ranging between 2 to 3 mAs and 60 to 70 kVp, depending on skull thickness and on specific anatomical variations such as the sagittal crest.

Image quality was fully adjusted for brightness and contrast, and all radiographs were exported in JPEG format. Metal detection was descriptive and based on the identification of metal opaque elements.

Computed Tomography—A General Electric Bright Speed 16-row CT scanner (General Electric Medical Systems, Milwaukee, WI, USA) was used. Skulls were scanned independently or two per scan and then placed in ventral recumbency (Figure 3). For positioning purposes, foam wedges were used. The scans were acquired and extended from the rostral aspect of the head to the occipital condyles. Scans were performed in helical acquisition mode with a field of view of 16 cm, scan thickness of 0.5 mm, a pitch of 1.5:1, 80 to 250 mAs, 120 kVp, tube rotation time of 0.6 s, and a 512 × 512 matrix. Images were reconstructed into a transverse plane using a bone algorithm. The slice thickness of the reformatted images was 1.25 mm, and the display field of view was tailored to the size of the skull. A higher mAs was required for the skull of large adult

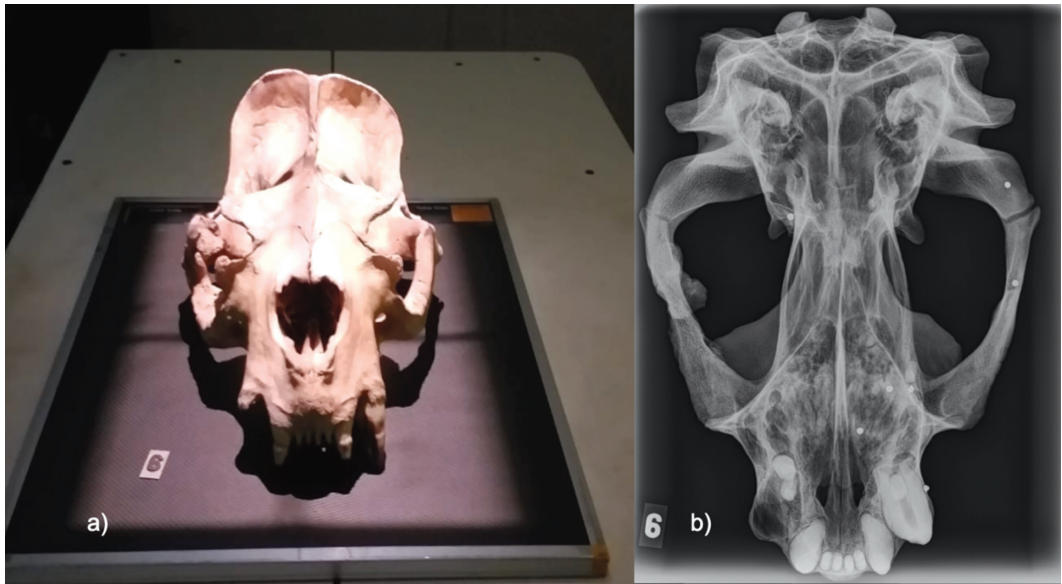


Figure 1. Positioning and dorsoventral digital radiograph of a pinniped skull: (a) positioning of a South American sea lion (*Otaria byronia*) skull on the radiographic image detector to obtain a dorsoventral view; and (b) dorsoventral digital radiograph of an *O. byronia* skull.

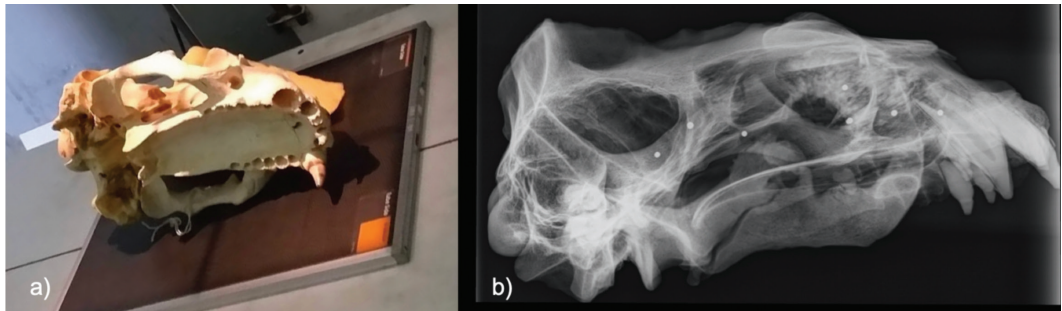


Figure 2. Positioning and lateral digital radiograph of a pinniped skull: (a) positioning of a South American sea lion skull on the radiographic image detector to obtain a lateral view; and (b) lateral digital radiograph of an *O. byronia* skull.

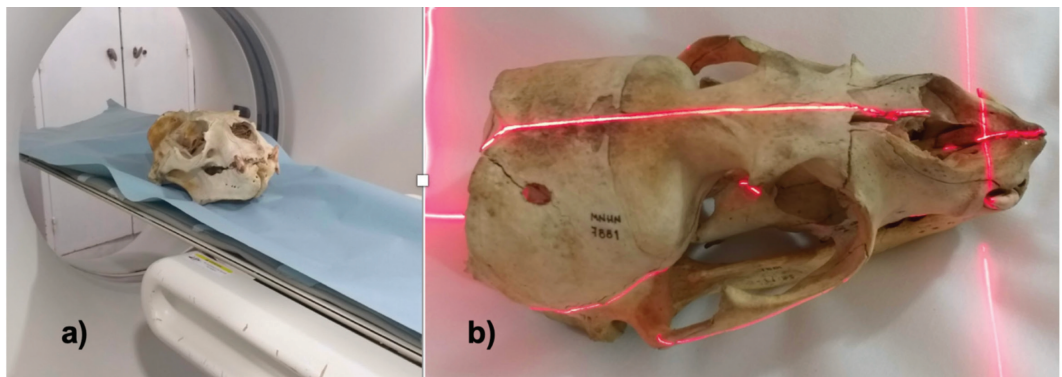


Figure 3. (a) Pinniped skull of a South American fur seal (*Arctocephalus australis*) positioned in ventral recumbency on the CT table; and (b) laser indicating the midline of the skull that was used for centering the skull.

male sea lions to maintain the image quality due to the increase in head size, the thickness of the bones, and the bigger sagittal crest.

CT examinations were viewed using two different commercially available imaging softwares: (1) *Merge PACS*[™] (IBM Watson Health, Cambridge, UK; FVG and AWS) and (2) the 164-bit version of *RadiAnt DICOM Viewer*, Version 5.0 (Medixant, Poznań, Poland; VS). The images were reviewed in the transverse plane using modified window settings (350 to 450 WL and 4,000 WW). The detection of metal fragments was based on the identification of fragments with an attenuation greater than $2,200 \pm 3,000$ Hounsfield Units (HU) (Amadasi et al., 2013; Paulis et al., 2019) and having associated metal-related CT artifacts. These metal-related CT artifacts are called beam hardening, scattering, and Poisson noise. Beam hardening and scattering result in dark streaks between the metal with surrounding bright streaks (Boas & Fleischmann, 2012). For assessing attenuation, a closed polygon tool was used to manually trace a region of interest, including the entire metal fragment (Figure 4). For smaller metal fragments, a probe tool was used which allowed us to peek at the pixel coordinates of the location under the cursor and to determine the actual HU value of that pixel.

All images were retrospectively reviewed by a veterinarian (VS), a board-certified veterinary radiologist (FVG), and a board-certified veterinary pathologist (AWS). Observers were blinded to any patient and imaging information. A data collection sheet was prepared using *Microsoft Excel* software (Microsoft Office, Albuquerque, NM, USA). The observers answered affirmatively or negatively for the presence of metal fragments with each imaging technique. If metal fragments were observed, the number of identified fragments was also recorded with each imaging technique.

Statistical Analysis

The presence of metal fragments was compared between the different observers for the same imaging technique (DR and CT) using Fisher's Exact test. The differences in the presence of metallic fragments between DR and CT, obtained from the three observers for each skull in each imaging technique, was analyzed using the McNemar test; and the number of metallic fragments recorded by each observer were analyzed separately according to the imaging technique (DR or CT) by the Kruskal-Wallis test. Comparisons of the number of metallic fragments recorded by DR and CT using the average obtained from the three observers in each technique were analyzed by the Wilcoxon test.

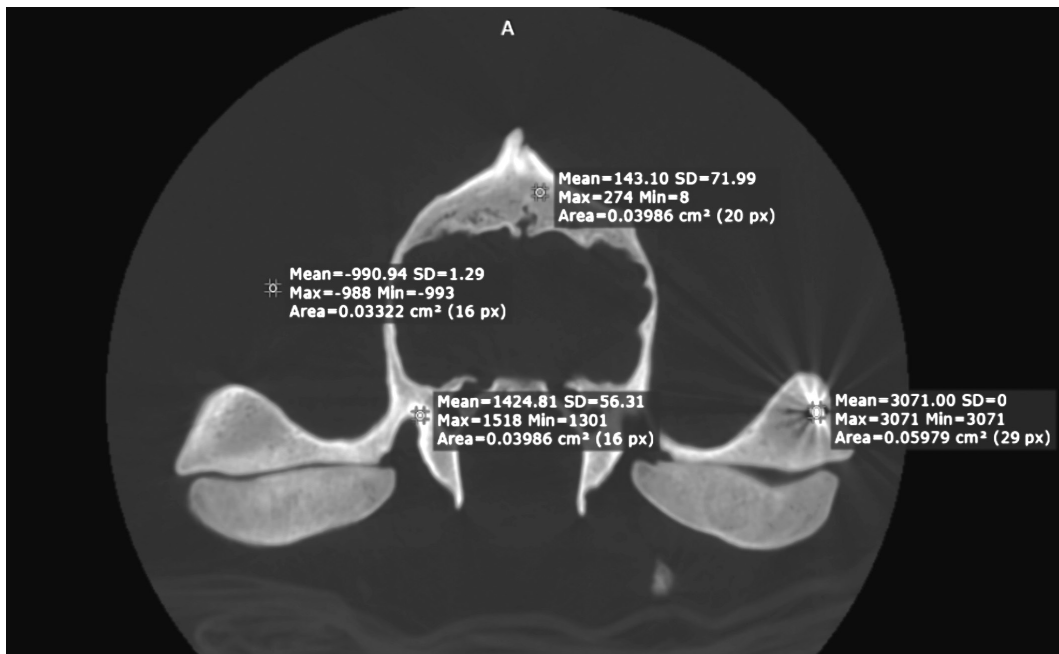


Figure 4. Cross-sectional cutting thicknesses of 1.25-mm CT image of a South American sea lion. Representation of the different attenuations present in the image and their average value in Hounsfield Units (HU). In this skull, the metallic fragment identified had an attenuation value of 3,071.00 HU; the cortical bone, 1,424.81 HU; the spongy bone, 143.10 HU; and air, -990.94 HU. Note the metal-related artifacts associated with the metallic fragment.

The Fleiss kappa method was used to evaluate the level of agreement between the three evaluators on a categorical scale (presence or absence of metal fragments) for the same technique, which is an extension of the Cohen's Kappa method (Fleiss et al., 2003). The Cohen's Kappa method (Cohen, 1968) was used to evaluate the level of agreement between DR and CT using the results obtained from the three observers for each skull in each technique. Results were considered significant at $p \leq 0.05$. Data on the number of metal fragments are presented as mean \pm standard error of mean.

Results

The presence of metal fragments in pinniped skulls for each of the techniques was not different between observers ($p = 1.0$). Using DR, all observers detected the presence of metal fragments in 13 animals (Figure 5); and using CT, all observers detected the presence of metal fragments in 16 skulls (Figure 6).

Different types of projectiles can be identified according to their shape and size—for example, a spherical projectile, such as a ball bearing (BB), used by shotguns and air guns (Figure 7). The presence of metal fragments in pinniped skulls was not significantly different between DR (13/30) and CT (16/30) techniques ($p = 0.71$). The degree of agreement between the two techniques was excellent and significant.

There was no difference between observers in the number of metal fragments detected by DR (observer 1: 6.0 ± 1.6 ; observer 2: 7.6 ± 2.1 ; observer 3: 6.2 ± 2.1 ; $p = 0.79$); there was no difference between observers in the number of metal fragments detected by CT (observer 1: 9.6 ± 2.1 ; observer 2: 8.3 ± 1.9 ; observer 3: 7.5 ± 1.7 ; $p = 0.75$); and the number of metal fragments in pinniped skulls was not significantly different between DR (6.6 ± 1.9) and CT (7.9 ± 1.7) ($p = 0.37$).

There was an excellent agreement between the three observers for DR (kappa = 1.0; $p < 0.0001$)



Figure 5. Dorsoventral radiographs of two pinnipeds: (a) South American fur seal—there is a small metal fragment in the occipital region (discontinuous arrow) and multiple skull fractures (solid arrow); and (b) South American sea lion—there are multiple round metal fragments in the left zygomatic region (arrowheads).

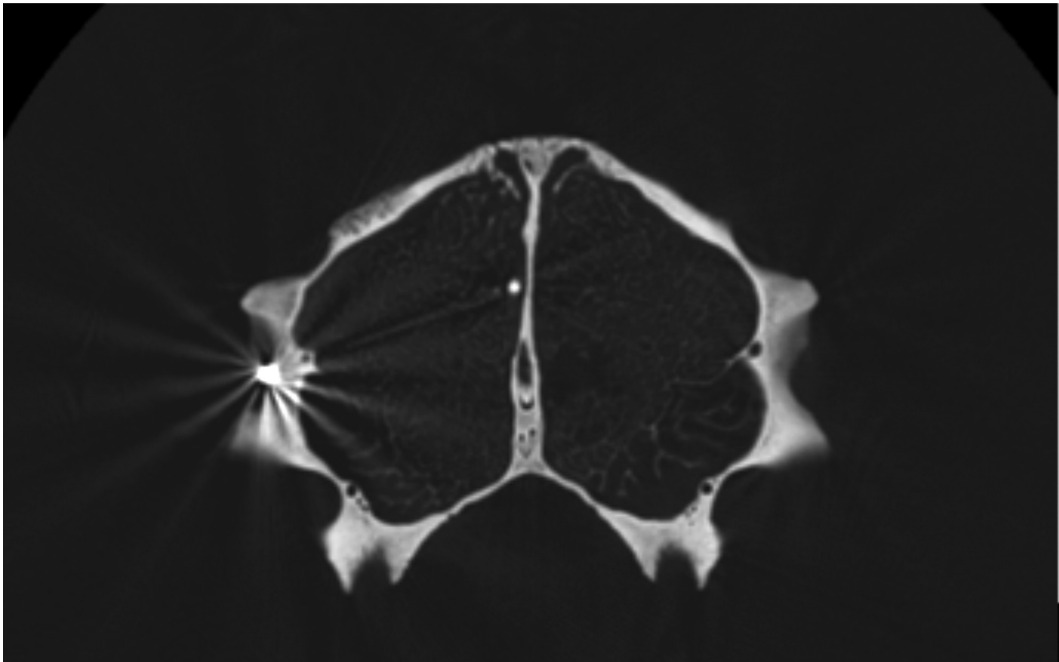


Figure 6. Transverse cutting thicknesses of 1.25-mm CT image reconstructed in a bone algorithm of a skull of a South American sea lion with presence of a metal fragment and the associated metal-related CT artifacts. Hypo- and hyperdense transition lines are centered on metallic objects.

and between the three observers for CT ($\kappa = 1.0$; $p < 0.0001$). There was also an excellent agreement between the two techniques (DR and CT: $\kappa = 0.802$; $p < 0.0001$).

Discussion

This study compared the effectiveness of DR and CT in detecting metal fragments. Goldstein et al. (1999) described that most of the injuries caused by projectiles resulted in the death of sea lions and were associated to a greater extent with the neck and/or the head. Coincidentally, the high number of sea lion skulls studied in the current study show similar lesions, revealing a high incidence of human interactions, which is why imaging techniques are essential for the investigation when projectile injuries are suspected.

Brogdon (1998) describes different types of bullets and their metallic composition, generating very different images on DR and CT. Depending on the type of ammunition used and the density of the target hit, the severity of the wound can increase and alter the fragmentation pattern of the bullet (Wilson, 1999; DiMaio, 2015). In the DR and CT images obtained in this study, we were able to observe the presence of multiple metal fragments with characteristics of

different shapes and sizes, as well as numerous bone fractures.

According to Dodd et al. (1990), we must consider that the number of bullets held in a body can be counted relatively easily unless fragmentation is excessive. In addition, the composition of the metal fragment determines whether it is visible in the image or not, and its size can influence the intensity and dimensions in the image. Because of all these factors, one projectile could not be identified by one method but was successfully detected by another (Aras et al., 2010).

In the current study, there were three cases in which metal fragments were detected using CT and not detected using DR. It is possible that the overlap of dense bone with metal fragments may have masked these small fragments from being identified in the radiographs. Additionally, the intrinsic resolution of the DR systems used may be limited when the metal fragment is too small. In this study, we only used orthogonal views; however, we hypothesize that additional oblique radiographic views could have revealed these fragments in these three skulls as described by Harcke et al. (2007) and Levy et al. (2010). Another limitation in the detection of metal fragments with DR may be due to the use of JPEGs instead of DICOM files since JPEGs do not allow for manipulation of the images.

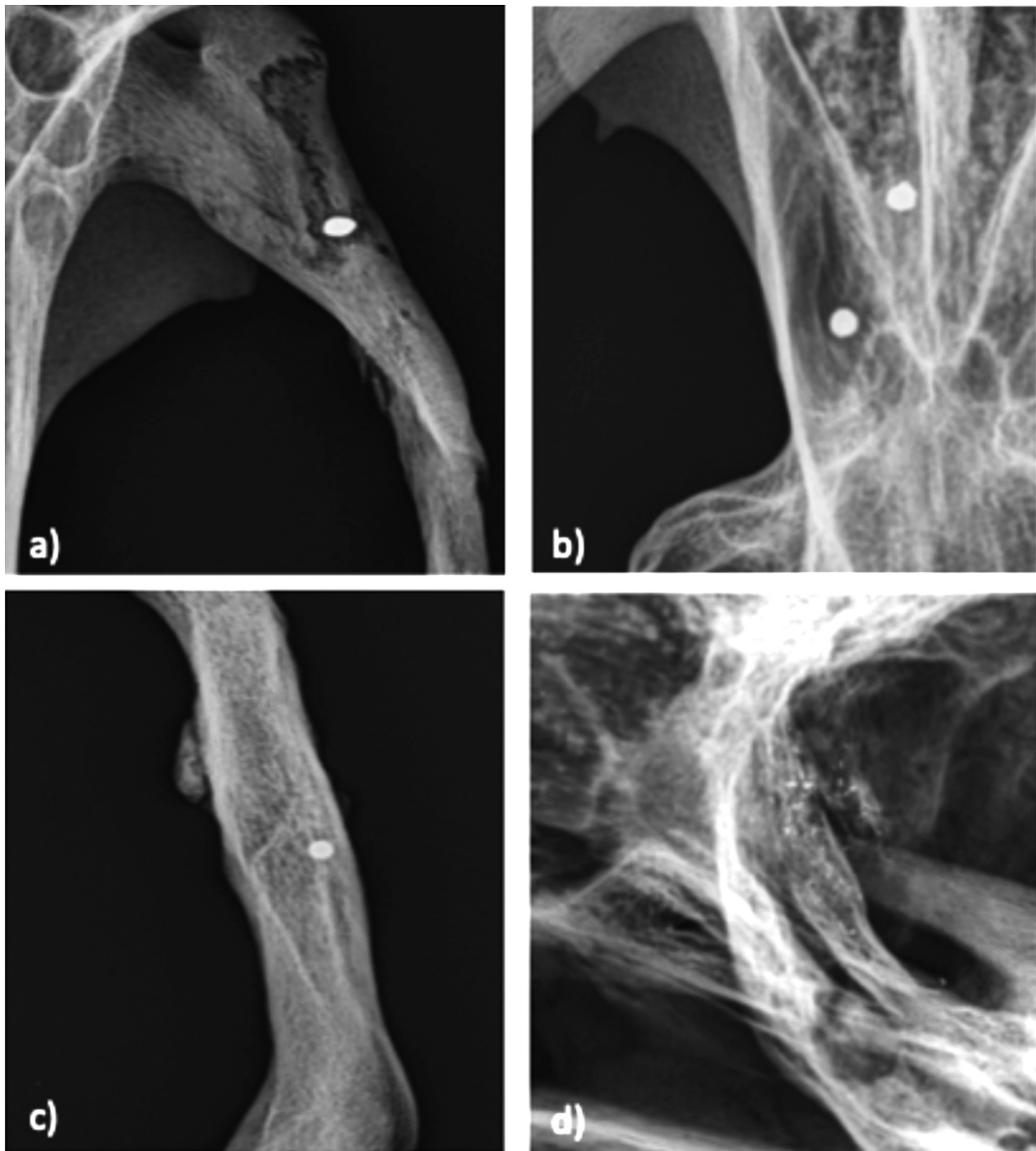


Figure 7. Examples of projectiles observed in pinniped skulls: (a) digital radiograph of a spherical BB in a South American fur seal; (b) digital radiograph of a spherical BB in a South American sea lion; (c) digital radiograph of a spherical projectile in a South American sea lion; and (d) digital radiograph of small metallic fragments in a South American fur seal.

Amadasi et al. (2013) compared the sensitivity of DR, CT, and magnetic resonance imaging (MRI) for the detection of metal fragments in previously burned bones and found that DR was more sensitive than CT. In that study, they suspected that this could be due to the use of 5-mm CT slice thickness as the metal fragments may become too small to be recognized in CT slices of this size. In our study, we followed the CT protocol

recommended by Fraga-Manteiga et al. (2014) for the assessment of head trauma in a seal model using 1.25-mm slice thickness, which allowed for the visualization of small metal fragments.

The current study showed that DR is a valid imaging technique for detecting metal fragments, although it can result in an underestimation of the actual number of metal fragments or it may not detect small metal fragments. In contrast,

CT is able to accurately detect and locate metal fragments, but its sensitivity depends to a large extent on the slice thickness used. It is important to understand the different diagnostic imaging techniques that can be used during forensic investigations of live and deceased animals, particularly the benefits and limitations of each imaging modality (Watson, 2018). Investigation of crimes against animals, including wildlife, requires both the correct equipment and proper techniques for each scenario. The use of DR is advantageous as some units are portable and are easy to use. As in a forensic case, an interdisciplinary approach is essential, and incorporation of imaging modalities into investigations would be beneficial to all investigators.

Conclusions

In this study, there was an excellent agreement between DR and CT in the detection and quantification of metal fragments in postmortem pinniped skulls, with no significant differences between both imaging techniques regardless of the observer's profession. However, CT was capable of detecting and identifying more metal fragments. Therefore, we recommend the use of DR as the first imaging technique to assess suspected projectile-related injuries in pinniped skulls.

Acknowledgments

The authors would like to thank Meica Valdivia of the Museo de Historia Natural del Uruguay for her valuable contribution and collaboration, Victoria Serrano of Hospital Maciel for the collaboration in the acquisition of the CT images, and Dr. Gonzalo Suárez for his guidance in statistical analysis.

Literature Cited

- Amadasi, A., Borgonovo, S., Brandone, A., Di Giancamillo, M., & Cattaneo, C. (2013). A comparison between digital radiography, computed tomography, and magnetic resonance in the detection of gunshot residues in burnt tissues and bone. *Journal of Forensic Sciences*, 59(3), 712-717. <https://doi.org/10.1111/1556-4029.12304>
- Aras, M. H., Miloglu, O., Barutcugil, C., Kantarci, M., Ozca, E., & Harorli, A. (2010). Comparison of the sensitivity for detecting foreign bodies among conventional plain radiography, computed tomography and ultrasonography. *Dentomaxillofacial Radiology*, 39(2), 72-78. <https://doi.org/10.1259/dmfr/68589458>
- Aso, J., Martínez-Quinones, J. V., Aso-Vizán, J., Pons, J., Arregui, R., & Baena, S. (2005). Virtopsy. Applications of a new method of non-invasive body inspection in forensic sciences. *Cuadernos de Medicina Forense*, 11(40), 95-106.
- Bastida, R., & Rodríguez, D. (2010). *Mamíferos marinos de Patagonia y Antártida* [Marine mammals of Patagonia and Antarctica]. Vazquez Mazzini.
- Boas, F. E., & Fleischmann, D. (2012). CT artifacts: Causes and reduction techniques. *Imaging in Medicine*, 4(2), 229-240. <https://doi.org/10.2217/iim.12.13>
- Brogdon, B. G. (1998). The scope of forensic radiology. *Clinics in Laboratory Medicine*, 18(2), 203-240. [https://doi.org/10.1016/S0272-2712\(18\)30169-0](https://doi.org/10.1016/S0272-2712(18)30169-0)
- Cárdenas, J. C. (2018). *Pesca artesanal y lobos marinos: Biopopulismo y crisis socio-ambiental en el mar de Chile* [Artisanal fishing and sea lions: Biopopulism and socio-environmental crisis in the Chilean sea]. www.eldesconcierto.cl/2018/10/20/pesca-artesanal-y-lobos-marinos-biopopulismo-y-crisis-socio-ambiental-en-el-mar-de-Chile
- Cohen, J. (1968). Weighted kappa: Nominal scale agreement provision for scaled disagreement or partial credit. *Psychological Bulletin*, 70(4), 213-220. <https://doi.org/10.1037/h0026256>
- Crespo, E. A., Sepúlveda, M., & Szteren, D. (2012). Interactions between the common sea lion and fishing and aquaculture activities. In E. A. Crespo, D. Oliva, S. Dans, & M. Sepúlveda (Eds.), *Status of the common sea lion in its range* (pp. 68-72). University of Valparaíso. ISBN 9789562141062
- DiMaio, V. J. M. (2015). Gunshot wounds. In V. J. M. DiMaio (Ed.), *Gunshot wounds: Practical aspects of firearms, ballistics, and forensic techniques* (Vol. 62, pp. 71-81). CRC Press. <https://doi.org/10.1201/b18888>
- Dodd, G. D., & Budzik, R. F., Jr. (1990). Identification of retained firearm projectiles on plain radiographs. *American Journal of Roentgenology*, 154(3), 471-475. <https://doi.org/10.2214/ajr.154.3.2106206>
- Fleiss, J., Levin, B., & Paik, M. (2003). *Statistical methods for rates and proportions* (3rd ed.). Wiley. 800 pp.
- Fraga-Manteiga, E., Shaw, D. J., Dennison, S., Brownlow, A., & Schwarz, T. (2014). An optimized computed tomography protocol for metallic gunshot head trauma in a seal model. *Veterinary Radiology & Ultrasound*, 55(4), 393-398. <https://doi.org/10.1111/vru.12146>
- Goldstein, T., Johnson, S. P., Phillips, A., Hanni, K. D., Fauquier, D. A., & Gulland, F. (1999). Human-related injuries observed in live stranded pinnipeds along the central California coast 1986-1998. *Aquatic Mammals*, 25(1), 43-51.
- Harcke, H. T., Levy, A. D., Abbott, R. M., Mallak, C. T., Getz, J. M., Champion, H. R., & Pearse, L. (2007). Autopsy radiography: Digital radiographs (DR) vs multidetector computed tomography (MDCT) in high-velocity gunshot-wound victims. *The American Journal of Forensic Medicine and Pathology*, 28(1), 13-19. <https://doi.org/10.1097/O1.paf.0000257419.92109.ce>
- Jefferson, T. A., Webber, M. A., & Pitman, R. L. (2015). *Marine mammals of the world: A comprehensive guide to their identification* (2nd ed.). Academic Press.
- Jeffery, A. J., Rutty, G. N., Robinson, C., & Morgan, B. (2008). Computed tomography of projectile injuries. *Clinical*

- Radiology*, 63(10), 1160-1166. <https://doi.org/10.1016/j.crad.2008.03.003>
- Levy, A. D., Harccke, H. T., & Mallak, C. T. (2010). Postmortem imaging: MDCT features of postmortem change and decomposition. *The American Journal of Forensic Medicine and Pathology*, 31(1), 12-17. <https://doi.org/10.1097/PAF.0b013e3181c65e1a>
- Listos, P., Komsta, R., Lopuszyński, W., Gryzińska, M., Teresiński, G., Chagowski, W., Buszewicz, G., & Dylewska, M. (2016). Radiological and forensic veterinary analysis of gunshot cases in eastern Poland. *Medycyna Weterynaryjna*, 72, 453-457. <https://doi.org/10.21521/mw.5531>
- Montes Loaiza, G. A., Otálora Daza, A. F., & Archila, G. A. (2013). Applications of conventional radiology in the medical-forensic field. *Revista Colombiana de Radiología*, 24(4), 3805-3817.
- Motta-Ramírez, G. A., Alva-Rodríguez, M., & Herrera-Avilé, R. A. (2013). La autopsia virtual (virtopsia): La radiología en la medicina forense [The virtual autopsy (virtopsia): Radiology in forensic medicine]. *Revista Sanidad Militar*, 67(3), 115-123.
- Munro, R., & Munro, H. M. C. (2013). Some challenges in forensic veterinary pathology: A review. *Journal of Comparative Pathology*, 149(1), 57-73. <https://doi.org/10.1016/j.jcpa.2012.10.001>
- Newbery, S., & Munro, R. (2011). Forensic veterinary medicine: 1. Investigation involving live animals. *InPractice*, 33(5), 220-227. <https://doi.org/10.1136/inp.d2876>
- Paulis, L. E., Kroll, J., Heijnsens, L., Huijnen, M., Gerretsen, R., Backes, W. H., & Hofman, P. A. M. (2019). Is CT bulletproof? On the use of CT for characterization of bullets in forensic radiology. *International Journal of Legal Medicine*, 133(6), 1869-1877. <https://doi.org/10.1007/s00414-019-02033-0>
- Read, A. J., & Murray, K. T. (2000). *Gross evidence of human-induced mortality in small cetaceans* (NOAA Technical Memorandum NMFS-OPR-15). National Oceanic and Atmospheric Administration, U.S. Department of Commerce. 21 pp.
- Ribas, L. M., Massad, M. R., Tremori, T. M., Reis, S. T., Eising, T. C., & Rocha, N. S. (2015). Postmortem analysis of injuries by roadkill of a white-eared opossum (*Didelphis albiventris*) by radiographs and forensic necropsy: A virtopsy case report. *Journal of Veterinary Science & Technology*, 7(1). <https://doi.org/10.4172/2157-7579.1000282>
- Singal, K. (2015). History and modalities of forensic radiology: A review. *Austin Journal of Forensic Science and Criminology*, 2(5).
- Stein, K. M., Bahner, M. L., Merkel, J., Ain, S., & Mattern, R. (2000). Detection of routine TC shooting residues. *International Journal of Legal Medicine*, 114(1-2), 15-18. <https://doi.org/10.1007/s004149900124>
- Thali, M. J., Kneubuehl, B. P., Bolliger, S. A., Christe, A., Koenigsdorfer, U., Ozdoba, C., & Dirnhofer, R. (2007). Forensic veterinary radiology: Computed tomographic 3D ballistic-radiological reconstruction of an illegal shooting of lynx in Switzerland. *Forensic Science International*, 171(1), 63-66. <https://doi.org/10.1016/j.forsciint.2006.05.044>
- Watson, E. (2018). Veterinary forensic radiology and imaging. In E. Rogers & A. W. Stern (Eds.), *Veterinary forensics: Investigation, evidence collection, and expert testimony* (pp. 251-272). CRC Press. <https://doi.org/10.4324/9781315153421-9>
- Watson, E., & Heng, H. G. (2017). Forensic radiology and images for veterinary radiologist. *Veterinary Radiology & Ultrasound*, 58(3), 245-258. <https://doi.org/10.1111/vru.12484>
- Wilson, A. J. (1999). Gunshot injuries: What does a radiologist need to know? *Radiographics*, 19(5), 1358-1368. <https://doi.org/10.1148/radiographics.19.5.g99se171358>